Time-resolved spectroscopy for $5s'^4D_{7/2}$ state transitions undergoing electron–ion recombination in femtosecond laser-produced copper plasma*

Hai-Ying Song(宋海英)[1], Hui Li(李辉)[1], Yan-Jie Zhang(张艳杰)[1], Peng Gu(谷鹏)[1], Hai-Yun Liu(刘海云)[1], Wei Li(李维)[2], Xun Liu(刘勋)[2], and Shi-Bing Liu(刘世炳)[1,†]

[1] *Strong-field and Ultrafast Photonics Laboratory, Institute of Laser Engineering, Beijing University of Technology, Beijing* 100124, *China*
[2] *Beijing Institute of Space Mechanics and Electricity, China Academy of Space Technology, Beijing* 100094, *China*

(Received 21 June 2017; revised manuscript received 31 July 2017; published online 20 October 2017)

In the femtosecond laser-produced Cu-plasma, the transient transition dynamics that the excited state $5s'^4D_{7/2}$ via electron–ion recombination transfers to $4p'^4F^0_{9/2}$ (465.11 nm, Λ_1 line) and $4p'^4D^0_{7/2}$ (529.25 nm, Λ_2 line) states are investigated by using the time-resolved spectroscopy. The occupation number and relevant lifetime of the excited state $5s'^4D_{7/2}$, the temporal evolutions of spectral intensities for Λ_1 line and Λ_2 line emissions are demonstrated to be in direct proportion to the employed laser intensity, which reveals the transient features of transition dynamics clearly differing from that resulted in the traditional collision excitation. Furthermore, some unique characteristics for Λ_1 and Λ_2 transitions stemming from electron–ion recombination are examined in detail.

Keywords: time-resolved spectroscopy, recombination transition, laser-produced plasma

PACS: 42.50.Dv, 78.47.J–, 78.47.N– **DOI:** 10.1088/1674-1056/26/12/124208

1. Introduction

It is well known that the photochemistry in nature is exactly the chemistry of excited states by photon pulses. Manipulation of the excited states lifetime of atoms/molecules in various atmospheres is a gordian technique for the future development of photochemical reactions, since it involves many applied fields such as biopharmaceutical and photochemical reactions.[1,2] In recent decades, numerous efforts have been devoted to control the process of chemical reactions of atoms and molecules experimentally and theoretically.[3,4] However, most of these works focused on the photodissociation and photoionization of molecules by using femtosecond (fs) laser pluses,[5–9] for example, controlling the fragment ratio[10] and channels[11] in the dissociation and ionization processes, governing the orientation of diatomic molecules,[12] and probing the motion of dissociated and ionized electrons and ions.[13] The detailed processes in photodissociation or photoionization are of great significance for governing or controlling photochemical reactions. The relevant diagnoses of these ultrafast processes are usually carried out by using time-resolved measuring methods, in order to obtain the dissociation fragments and electronic momentum distributions.[7–14]

The time-resolved probe method has been widely used for the investigation of various ultrafast phenomena, such as the process of material ejection by time-resolved shadowgraph method,[15] the population of electron transition by time-resolved atom/molecule emission,[16] the ultrafast dynamics of electron transfer by fs-laser stimulated Raman spectroscopy,[17] the transient resonance line of Ca^+ in Ca plasma by time-resolved spectroscopy,[18] the enhancing redshift phenomenon by time-resolved photoluminescence spectrum,[19] and so on.

In this paper, we investigate the transition dynamics of the excited state $5s'^4D_{7/2}$ through two transfer channels, $5s'^4D_{7/2} \rightarrow 4p'^4F^0_{9/2}$ (Λ_1 transition, corresponding spectrum called Λ_1 line) and $5s'^4D_{7/2} \rightarrow 4p'^4D^0_{7/2}$ (Λ_2 transition, corresponding spectrum called Λ_2 line), in the electron–ion recombination of copper plasma produced by both linear and circular polarized fs-laser pulses with different laser energy in air. The Λ_1 line and Λ_2 line emitting spectra are obtained by an intensified CCD (ICCD) spectrometer with resolution of 1200 G/mm, based on which the relaxation of the excited state occupation in the process of electron–ion recombination is examined by probing the time evolution of the characteristic spectra from both transfer channels.

2. Experimental result and discussion

The experimental setup is equipped with a commercial fs-laser system (Ti: sapphire Micra 10 and regenerative amplifier Legend Elite-USP-HE, Coherent Corp.) with 60 fs pulse du-

*Project supported by the National Natural Science Foundation of China (Grant No. 51705009) and the NSAF of China (Grant No. U1530153).
†Corresponding author. E-mail: sbliu@bjut.edu.cn
© 2017 Chinese Physical Society and IOP Publishing Ltd

ration, central wavelength at 800 nm (1.55 eV), output energy of 3.5 mJ/pulse, and repetitive rate of 1 kHz. The spot size (diameter) of laser pulse irradiating on target surface is 100 μm, and the average power density (intensity) arrived at the target surface is about 6.37×10^{14} W/cm^2, which is shown schematically in Fig. 1.

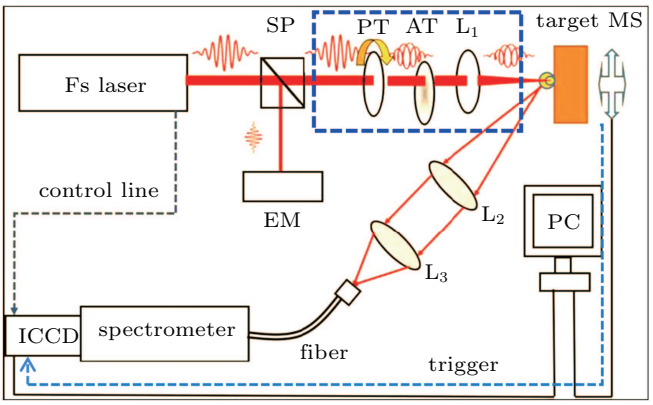


Fig. 1. (color online) Schematic diagram for experimental arrangement, where the components in the dashed frame are used for conversion of laser polarization state, SP is a beam splitter, EM is an energy meter used to detect the applied laser energy, AT is an attenuator for adjusting the pulse energy arrived at the target surface, $L_{1,2,3}$ are lenses, and MS is a two-dimensional (2D) motorized platform on which Cu sample is fixed.

In our laser-target experiment, fs-laser pulse is split into two beams, one is used to monitor the stability of output power and the other one used as pump light to produce plasma from the target. The detection unit is composed of lenses (L_2 and L_3), bandpass filter (800 nm), fiber, spectrometer, and ICCD camera (PI Corp., USA) with a basic gate width (i.e., exposure time for one triggering) of $\Delta\tau = 2$ ns. The ICCD is synchronized to the fs-laser pulse so as to perform all measurements of time-resolved spectra. The experiments were performed in the atmosphere.

2.1. Time-resolved measurement of spectra for two transfer channels

In the experiment, the employed linearly polarized laser energy is about 2.4 mJ (corresponding energy fluence ∼ 30 J/cm^2), the moment that the normal incident laser pulse arrives at the target surface is set as $t = 0$. The time evolution of emitted spectral intensities from both channels of Λ_1 line and Λ_2 line in the process of electron–ion recombination are shown in Fig. 2. It is well known that electron–ion interaction plays a significant role after laser-induced ionization process and immediately ample continuous spectra (CS) emission occur due to the bremsstrahlung process of electron–ion collision as well as recombination radiation between continuous states in atoms,[20,21] etc.

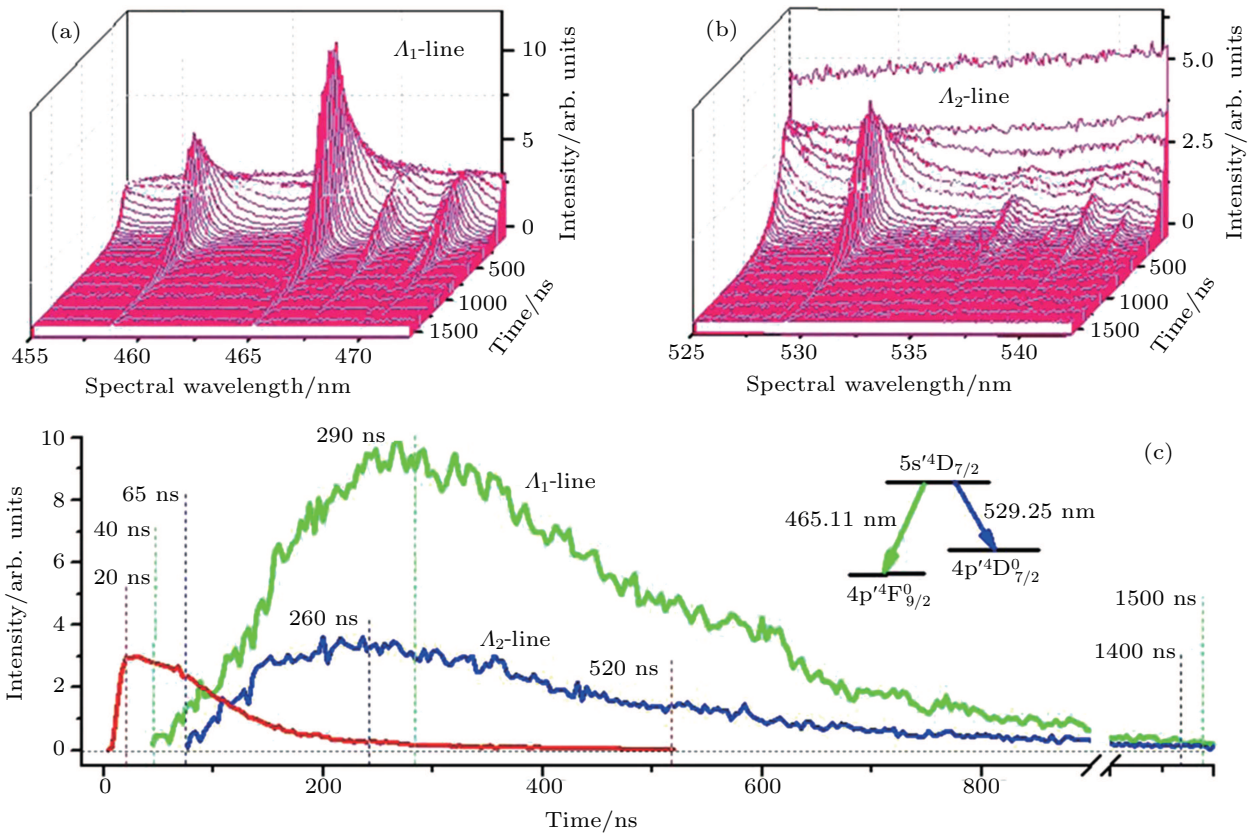


Fig. 2. (color online) Time-evolution of emitted spectral intensities from fs laser-produced plasma in the spectral windows (a) from 455 nm to 475 nm, (b) from 525 nm to 540 nm, and (c) continuous spectra (CS), Λ_1 line (465.11 nm), and Λ_2 line (529.25 nm) where the inset is the relevant energy level transition diagram for Λ_1 line and Λ_2 line emissions.

Figures 2(a) and 2(b) show the continuous spectrum and characteristic spectral lines of Λ_1 line and Λ_2 line by time-resolved measurement with ICCD spectrograph. The characteristic Λ_1 line appears at wavelength 465.11 nm and results from transition radiation of $5s'^4D_{7/2} \rightarrow 4p'^4F^0_{9/2}$, Λ_2 line appears at wavelength 529.25 nm and results from transition radiation of $5s'^4D_{7/2} \rightarrow 4p'^4D^0_{7/2}$, which is confirmed by comparison with the National Institute of Standards and Technology (NIST) Spectroscopic Properties of Atoms and Atomic Ions Database.[22] The time evolutions of continuous spectrum and Λ_1 and Λ_2 lines are extracted from data and shown in Fig. 2(c). One can see that the continuous spectrum peaks at about $t = 20$ ns prior to which it increases rapidly and decreases tardily after $t = 20$ ns. As is well known, the continuous spectrum or plasma spectrum results from the bremsstrahlung process (electro-ion collision)[23] including the recombination radiation within atomic continuous states and associated with the plasma distribution which is unquestionably dependent on the profile of laser intensity distribution. Therefore, in a Gaussian or Gaussian-like pulse the laser-produced plasma density increases rapidly before it peaks at 20 ns due to the processes of laser-ionization and energy absorption and decays relaxedly after peak value due to the free expansion. We can see also from Fig. 2(c) that first characteristic line, Λ_1 line, starts to appear at 40 ns and peaks at 290 ns, which means a pure plasma state with age (lifetime, here defined as the time of full width at 1/e maximum spectral intensity) of 40 ns and may accompany the spectral emission of recombination transition within atomic continuous states. The second characteristic line, Λ_2 line, starts to appear at 65 ns and peaks at 260 ns, which shows Λ_1 emitting antecedent to Λ_2 for 25 ns and peaking posterior to Λ_2 for 30 ns. The occupation number on the excited state $5s'^4D_{7/2}$ is piled up rapidly before 40 ns and then consumed successively by transition radiations of Λ_1 line and Λ_2 line, and the lifetime of Λ_1 line is larger than that of Λ_2 line. The results in Fig. 2(c) also indicate that the occupation number (particle number) on the excited state $5s'^4D_{7/2}$ mainly transfers to $4p'^4F^0_{9/2}$ state, which seems to be attributed to the energy level of $4p'^4F^0_{9/2}$ state inferior to that of $4p'^4D^0_{7/2}$ state.

Interestingly, from Ref. [24] we note that the lifetime of $5s'^4D_{7/2}$ generated by collision excitation of atoms is 10.7 ns theoretically and 7.9 ± 0.5 ns experimentally, which is obviously much shorter than that by laser-produced plasma. This significant difference may derive from that, we infer, the plasma produced by laser pulse possesses higher internal energy by absorbing laser energy and consequently the relaxation time of plasma state significantly lengthens which makes the rate of recombination transition to ease up. To reveal the distribution of occupation number on the excited state $5s'^4D_{7/2}$, the experimental curves of Λ_1 and Λ_2 lines are fitted numerically and found that the occupation number on $5s'^4D_{7/2}$ state approximates to Boltzmann distribution

$$I(t) = I_{\max} - \frac{I_{\max} - I_{\min}}{1 + \exp\left[(t - t_0)/(\mathrm{d}t)\right]}, \qquad (1)$$

where $I_{\max}$ and $I_{\min}(\sim 0)$ are maximum and minimum values of the spectral intensity, respectively, and t_0 is the time that spectrum stating emission. The slopes of rising and falling for spectral intensities of Λ_1 and Λ_2 lines are shown in Fig. 3, which further demonstrate the cumulative rate larger than the consumptive rate for the occupation number on the excited state $5s'^4D_{7/2}$. This result is straightforward for the distribution of occupation number on the excited state $5s'^4D_{7/2}$ because an intense Gaussian or Gaussian-like pulse laser generally gives rise to a Boltzmann or Boltzmann-like distribution of plasma numbers (electrons) and consequentially this Boltzmann-plasma also results in recombination transition rate to approximate Boltzmann distribution.

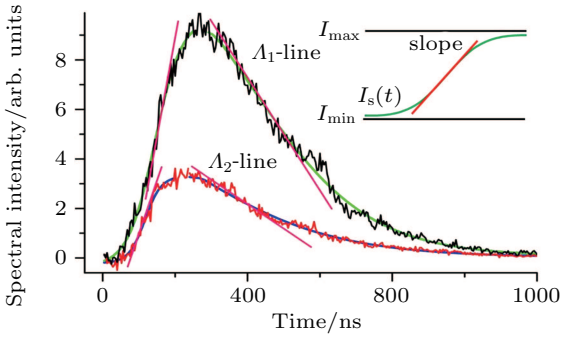


Fig. 3. (color online) Fitted time-evolution curves for spectral intensities of Λ_1 line and Λ_2 line emissions. Here the spectral curves rising and falling slopes are labeled by the red straight lines and the fitted curves are shown in smooth blue and green curves.

2.2. Dependence of emission spectra on laser intensity

In fs laser-produced plasma, the ionized electron energy depends closely upon employed laser intensity. To examine the dependence of electron energy on the spectral lifetime of transition radiation as well as the occupation number of excited states, we use different laser intensities to produce Cu-plasma. The time-resolved spectra for Λ_1 line and Λ_2 line and the CS under different laser intensities are shown in Fig. 4. It clearly shows that, from Fig. 4(a) and 4(b), the wavelengths of spectral peak intensity for both Λ_1 line and Λ_2 line undergo red-shift when laser intensity increases and, meanwhile, the spectra lifetimes increase proportionally. From Fig. 4(c), we can see interestingly that the peak positions of CS spectra nearly keep invariability still at 20 ns, while relevant lifetimes of CS are lengthened which no doubt is directly proportional to the employed laser intensity as well as associates with the electron energy (or internal energy of plasma).

More importantly, the start times of spectral emissions for Λ_1 line and Λ_2 line are still kept at $t = 40$ ns and 65 ns, respectively, and seem to show an independence on that employed laser intensity. It is worth noting that, from the above experimental data, with the increase of the employed laser intensity the peaks of the spectra evolution for CS appears invariably at 20 ns and the start times of spectral emissions from these two transition channels (Λ_1 and Λ_2 emissions) still remain at 40 ns and 65 ns, respectively, which seems to be difficult to interpret in physics and hence remains to be further investigated in our subsequent works.

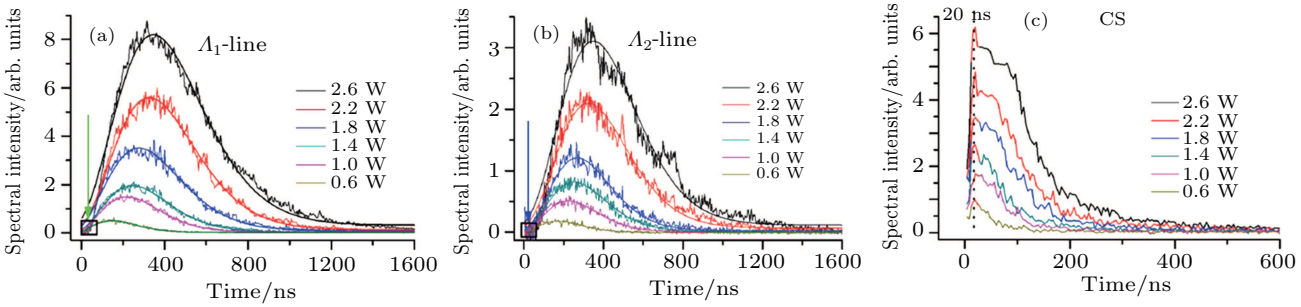


Fig. 4. (color online) Temporal evolution of spectra emissions for (a) Λ_1 line, (b) Λ_2 line, and (c) continuous spectra (CS) undergoes different laser powers (intensities).

Figure 5(a) shows the lifetimes of Λ_1 line and Λ_2 line emissions undergone by different laser intensities and observably exhibit linear dependence, while the fitted-lines also imply that the spectral peak intensity (SPI) emitting from Λ_1 and Λ_2 transfer channels approximatively conform to a simple quadratic nonlinear relation with employed laser intensity. Figure 5(b) shows the temporal evolution of SPI with different laser intensity, where the corresponding fitted curves are marked by green line for Λ_1 line and blue line for Λ_2 line. At the same probing time, the radio of Λ_1 line SPI to Λ_2 line SPI with the employed laser intensities are shown in Fig. 5(c) in which the data are extracted from Fig. 5(b). According to Ref. [22], the transition probability of Λ_1 transfer channel is 3.49 times that of Λ_2 transfer channel. Meanwhile in our experiment, from Fig. 5(c), the ratio of Λ_1 line SPI to Λ_2 line SPI is about 3.5 which coincidentally associates with the transition probability.

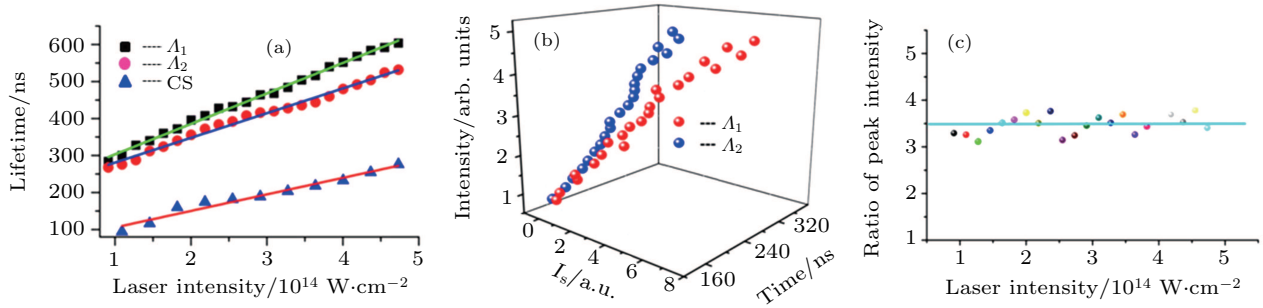


Fig. 5. (color online) Dependence of spectral property on laser intensity. (a) Spectral lifetimes of Λ_1 line and Λ_2 line, and CS, where the solid lines are corresponding numerical fitted-lines. (b) Spectral peak intensities (I_s) of Λ_1 line and Λ_2-line. (c) Ratio of spectral peak intensities of Λ_1 line to Λ_2 line in panel (b).

2.3. Effect of fs laser polarization state on spectral property

In the above experiments, the employed fs laser pulse remained in a linearly polarized state. To examine the dependence of spectral property on laser polarization state, we use a circular polarized fs laser pulse to impinge on a Cu-target, for which a 1/4 wave plate (PT in Fig. 1) was inserted in the incident light path so as to generate a circular polarized laser beam. In the experiments, all the other laser parameters were kept consistent except the polarization state of laser pulse, and for convenience as shown in Fig. 6, two laser powers of 2.4 W and 1.8 W were chosen for the comparison of spectral intensities in both linear and circular polarization states. It clearly shows that the spectral intensities induced by circular polarized light are stronger than that by linear polarized light, where Figs. 6(a)–6(b) for Λ_1 line and 6(d)–6(e) for Λ_2 line. According to the ponderomotive potential of an electron in laser field,[25,26] i.e.,

$$U_{\mathrm{p}}\,[\mathrm{eV}] = \frac{e^2 E_{\mathrm{L}}^2}{4 m_{\mathrm{e}} \omega_{\mathrm{L}}^2}\,(1+\alpha^2) \approx 9.33 \times 10^{-14} \times (1+\alpha^2) I_{\mathrm{L}} \lambda_{\mathrm{L}}^2, \tag{2}$$

one can find that the ponderomotive energy of an electron in the circular polarized laser field is twice as much as that in the linear polarized laser field, where α characterizes the polarization state of laser pulse (i.e., $\alpha = 1, 0$ for circular and linear polarized states, respectively), E_{L} is intensity of laser electric field, I_{L} [W/cm^2] is laser intensity, λ_{L} [μm] is laser wavelength. As is well-known in physics, the higher ponderomotive energy results in the more electron kinetic energy and thus the recombination rate of electron–ion as well as the transition rate increase which consequentially leads to an enhanced spectral intensity. Figures 6(c) and 6(f) represent the fitted curves of the spectral lifetimes for Λ_1 line and Λ_2 line associated with circular and linear polarized

states of laser pulse at different intensities. The same as the above discussed case on evolution of spectral intensity, in the circular polarization state the spectral lifetimes of Λ_1 line and Λ_2 line also show an evident increase in comparison with the case of the linear polarized laser pulse.

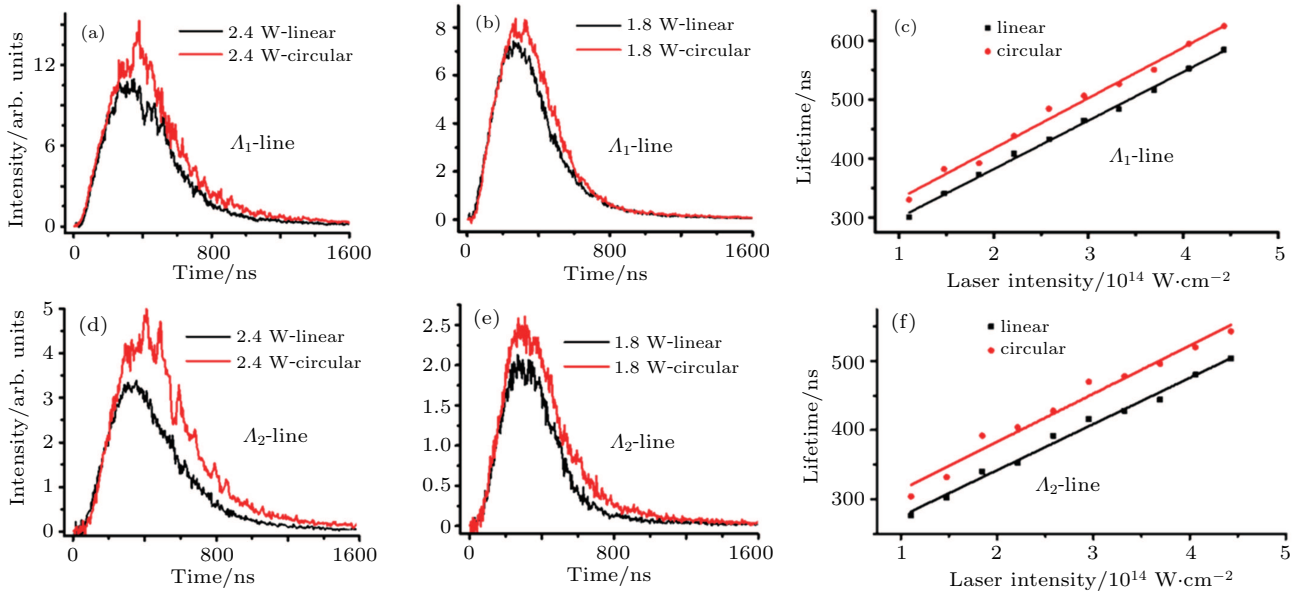


Fig. 6. (color online) Comparison of both linear and circular polarized states of laser pulse for the emitted spectral intensities and occupied lifetimes under different laser power, where the evolutions of spectral intensity are shown in panels (a)–(b) for Λ_1 line emission and panels (d)–(e) for Λ_2 line emission, and the fitted lines for occupation lifetimes on the excited state $5s'^4D_{7/2}$ are represented in panel (c) for Λ_1 transition and panel (f) for Λ_2 transition.

3. Conclusion

In conclusion, the transient transition dynamics for the excited state $5s'^4D_{7/2}$ generated by electron–ion recombination in fs laser-produced Cu plasma have been examined by time-resolved spectroscopy. The experimental results demonstrate that, 1) the particle occupation on the excited state $5s'^4D_{7/2}$ likely begins from 20 ns when the plasma CS peaks, 2) the characteristic spectra emissions or transitions to $4p'^4F^0_{9/2}$ state and $4p'^4D^0_{7/2}$ state start from 40 ns for Λ_1 line and 65 ns for Λ_2 line, respectively, 3) the above special times are confirmed as independence of employed laser intensity, 4) the time evolution of occupation number on the excited state $5s'^4D_{7/2}$ shows a Boltzmann role and mainly transfer to $4p'^4F^0_{9/2}$ state of lower energy level, 5) the lifetime of occupation on the excited state $5s'^4D_{7/2}$ resulting from the electron–ion recombination in laser-produced plasma is far longer than that in the traditional collision excitation, and 6) the dependence of SPIs for Λ_1 line and Λ_2 line emissions on employed laser intensity nearly accords with a quadratic nonlinear relation and the ratio of Λ_1 line SPI to Λ_2 line SPI approaches to 3.5 which interestingly meets 3.49, the ratio of transition probabilities of Λ_1 to Λ_2 at the same probing time.

References

[1] Rose T S, Rosker M J and Zewail A H 1989 *J. Chem. Phys.* **91** 12
[2] Tamura H and Nanbu S 2006 *J. Chem. Phys.* **125** 034307
[3] Yonehara T and Takatsuka K 2009 *Chem. Phys.* **366** 115
[4] Kraus P M, Schwarzer M C and Schirmel N 2011 *J. Chem. Phys.* **134** 114302
[5] Xie X and Doblhoff-Dier K 2012 *Phys. Rev. Lett.* **109** 243001
[6] Liu Y, Liu X and Deng Y 2011 *Phys. Rev. Lett.* **106** 073004
[7] Liu Y, Fu L, Ye D and Liu J 2014 *Phys. Rev. Lett.* **112** 013003
[8] Song Y D, Chen Z, Yang X, Sun C K, Zhang C C and Hu Z 2013 *Chin. Phys. B* **22** 0103301
[9] Liu D D and Zhang H 2013 *Chin. Phys. B* **22** 0103103
[10] Brixner T 2003 *ChemPhysChem* **4** 418
[11] Znakovskaya I, Von den Hoff P, Marcus G and Zherebtsov S 2012 *Phys. Rev. Lett.* **108** 063002
[12] Xie X, Doblhoff-Dier K and Xu H 2014 *Phys. Rev. Lett.* **112** 163003
[13] Borot A, Malvache A, Chen X, Jullien A, Geindre J P, Audebert P, Mourou G, Quéré F and Lopez-Martens R 2012 *Nat. Phys.* **8** 416
[14] Zhang D D, Ni Q, Luo S Z, Zhang J, Liu H, Xu H F, Jin M X and Ding D J 2011 *Chin. Phys. Lett.* **28** 033301
[15] Joshi H C, Kumar A, Singh R K and Prahlad V 2010 *Spectrochimica Acta Part B: Atomic Spectroscopy* **65** 415
[16] Ahmed J B and Jaïdane N 2009 *Spectrochimica Acta Part B: Atomic Spectroscopy* **64** 442
[17] Zhang N, Zhu X, Yang J and Wang X 2007 *Phys. Rev. Lett.* **99** 167602
[18] Hoffman D P, Lee O P, Millstone J E and Chen M S 2013 *J. Phys. Chem. C* **117** 6990
[19] Li W, Jin P, Wang W Y, Mao D F, Pan X, Wang X L and Wang Z G 2017 *Chin. Phys. B* **26** 077802
[20] Liu S B, Liu Y, He R and Chen T 2010 *Acta Phys. Sin.* **59** 5382 (in Chinese)
[21] Gu P, Liu S B, Liu S, Song H Y 2014 *Appl. Surf. Sci.* **293** 80
[22] Kock M and Richter J 1968 *Canadian Journal of Philosophy* **69** 180
[23] Kruer W L 1988 *The Pyhsics of Laser Plasma Interaction* (Addison-Wesley)
[24] Cederquist H, Mannervik S, Kisielinski M and Forsberg P 1984 *Phys. Scr.* **T8** 104
[25] Gamaly E G, Rode A V, Luther-Davies B, Tikhonchuk V T 2002 *Phys. Plasmas* **9** 949
[26] Corkum P B, Burnett N H and Brunel F 1989 *Phys. Rev. Lett.* **62** 1259